GCAGS JOURNAL
A Publication of the Gulf Coast Association of Geological Societies
www.gcags.org

Characterization, Origin, and Significance of Carbonate Pulverulite: A Weathering Product of Microporous Strata

Robert G. Loucks[1], Zsófia Poros[2], and Hans G. Machel[3]

[1]*Bureau of Economic Geology, Jackson School of Geosciences, University of Texas at Austin, University Station, Box X, Austin, Texas 78713–8924, U.S.A.*

[2]*ConocoPhillips Company, 935 N. Eldridge Pkwy., Houston, Texas 77079, U.S.A.*

[3]*Department of Earth and Atmospheric Sciences, 1–26 Earth Sciences Bldg., University of Alberta, Edmonton, Alberta T6G2E3, Canada*

ABSTRACT

Pulverulite rock is a very porous and weakly-cemented fine-grained carbonate (commonly limestone, containing variable amounts of dolomite, or dolostone), and pulverulite powder is a very fine degradational product of the pulverulite rock. The rock and powder are produced by weathering of microporous carbonates. In the Texas Hill Country area surrounding Junction, Texas, on the Edwards Plateau, pulverulite rocks and powders are common and well exposed. From a number of roadcuts, we investigated the formation of pulverulite rock and powder by analyzing samples that represent the transition from intact and firm parent rock, to slightly-weathered rock, to pulverulite rock (strongly weathered), to pulverulite powder. The process that produced the transition from intact rock to pulverulite rock was dissolution by meteoric water of an initial microporous limestone. Pulverulite powder formed by breaking down weakly-lithified pulverulite rock by rain and possibly, in part, by freeze/thaw cycles, or a combination of the two. The force of recrystallization of dissolved carbonate also may have added to the breakdown of the parent rock. Pulverulite rock in the Texas Hill Country is composed predominantly of weakly-cemented microcrystalline calcite particles that are rounded and pitted by dissolution. Similar pulverulite rocks are seen in the Middle East, where they form portions of economical microporous hydrocarbon reservoirs beneath unconformities. Relict pulverulite powder in the ancient record is a criterion for subaerial weathering.

INTRODUCTION

Rose (1972) and Mueller (1975) noted a very fine, white to light gray, carbonate powder on Lower Cretaceous Fort Terrett and Segovia roadcuts and outcrops in the Junction area of Central Texas (Figs. 1 and 2). They interpreted this carbonate powder, which they termed *pulverulite*, as a weathering product and noted it could be either calcite or dolomite dominated (Fig. 3). Other researchers (e.g., Kahle, 2012) also applied the term to weathered, very soft, friable, porous rock (pulverulite rock). Rose (1972) and Mueller (1975) did not research the origin of pulverulite powder much beyond recognizing it as a weathering product. Rose (1972) suggested that it formed since the roadcuts were excavated during the 1950s and 1960s.

Research here focuses on the stages of development of pulverulite rock and powder and on the precursors that could produce them. Specific objectives of this paper are to (1) provide a description of pulverulite rock and powder, (2) define the paragenesis of the formation of pulverulite rock and powder, (3) identify rock types that weather to pulverulite rock and powder, (4) discuss whether pulverulite rock and powder can be preserved into the rock record, and (5) reflect on whether pulverulite rock and former powder (now lithified) can form porous zones at unconformities that may be hydrocarbon reservoirs.

An understanding of the origin and processes of pulverulite rock or powder formation will aid in understanding diagenetic processes at subaerial unconformities and whether pulverulite rock or powder can be an indicator of unconformities. Most importantly, pulverulite rock or powder may be a potential hydrocarbon reservoir type beneath unconformities.

Manuscript received January 31, 2018; revised manuscript received February 13, 2018; manuscript accepted May 11, 2018.

GCAGS Journal, v. 7 (2018), p. 79–92.

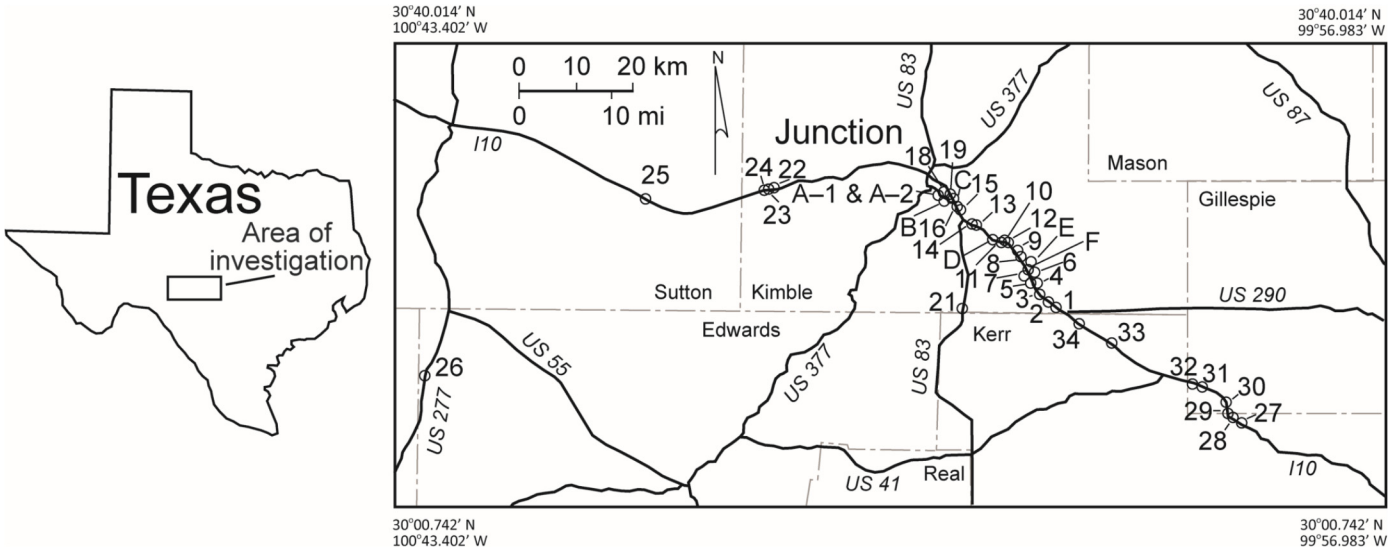

Figure 1. Area of investigation. Majority of samples were collected along Interstate 10.

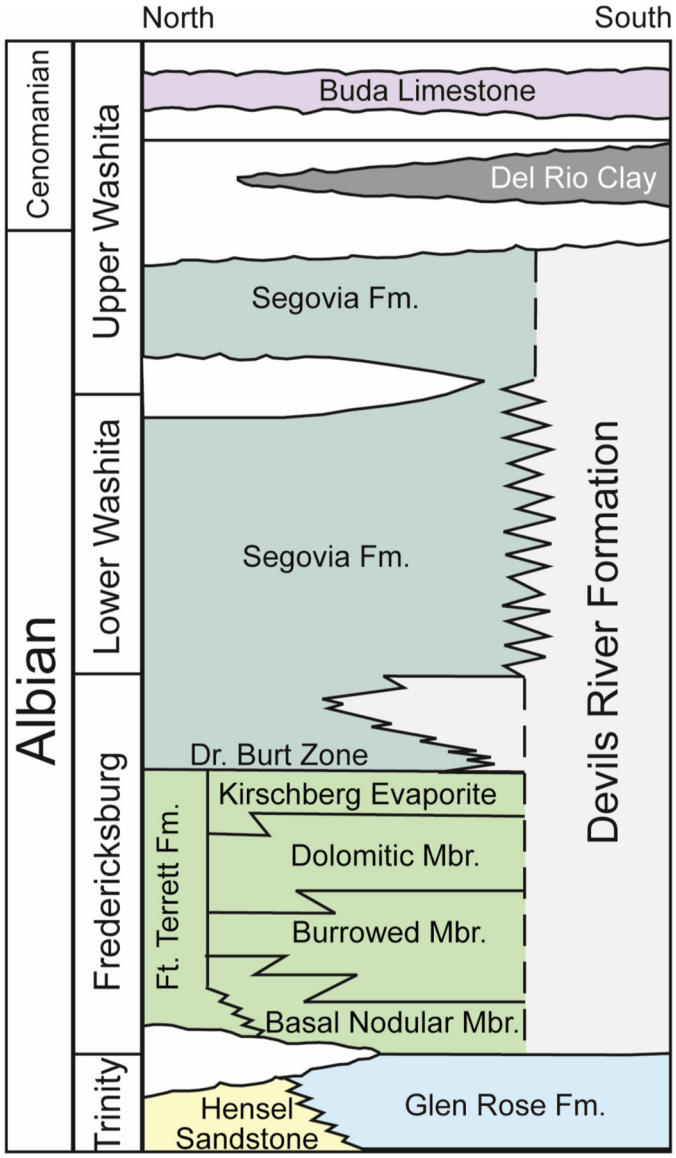

Figure 2. Stratigraphic section in the eastern part of the Edwards Plateau. Original section by Rose (1972), slightly modified by Mueller (1975) and present authors.

DATA AND METHODS

Lower Cretaceous roadcuts in the area of Junction, Texas (Fig. 1, Table 1), are the source of data for this investigation. Samples of intact host rock, weathered rock, and associated weathered powder were collected from 40 sites, mainly along Interstate 10 (generally younger roadcuts)—constructed between 1949 and 1968 in the Central Texas area (Wikipedia, 2017)—and adjoining service roads (generally older roadcuts). Care was taken to collect a spectrum of samples that represent the gradation of relatively unaltered strata to loose powder.

The firm rock samples were slabbed and investigated with a binocular microscope. Polished thin sections, stained for carbonate minerals, were prepared for 41 samples, including firm rock to very lightly lithified rock. The thin sections were impregnated with blue-dyed epoxy to highlight macropores and blue-fluorescent dye to highlight micropores under UV light. Loose powders were observed with a petrographic microscope by mounting the powder in oil on thin-section glass slides with a cover slip (Fig. 3D).

Semiquantitative X–ray diffraction (XRD) analysis was conducted on 34 pulverulite samples (Fig. 4), which were sieved through a 150-µm mesh screen. Approximately 15 mg of each powder sample were analyzed using an InXitu BTX 308 Portable XRD Analyzer at the University of Texas at Austin.

An additional 45 samples, ranging from relatively unaltered rocks to pulverulite powder, were analyzed for mineralogy by XRD at the University of Edmonton. Approximately 1 g of each sample was mixed with an internal quartz standard, then mounted on a zero-background plate. Samples were powdered using a low-speed microdrill with tungsten carbide and diamond bits. The equipment used was a Rigaku Ultima IV XRD system, which uses a cobalt tube with a radiation wavelength (λ) value of 1.78899Å, run at 40 kV and 35 mA. All scans were run from 2° to 100° 2θ, using a 0.02° 2θ step size with a scan speed of 2° 2θ per min. The resulting peaks were then corrected with the quartz internal standard d101 peak (31.035° 2θ). Minerals were identified with Jade 9 software.

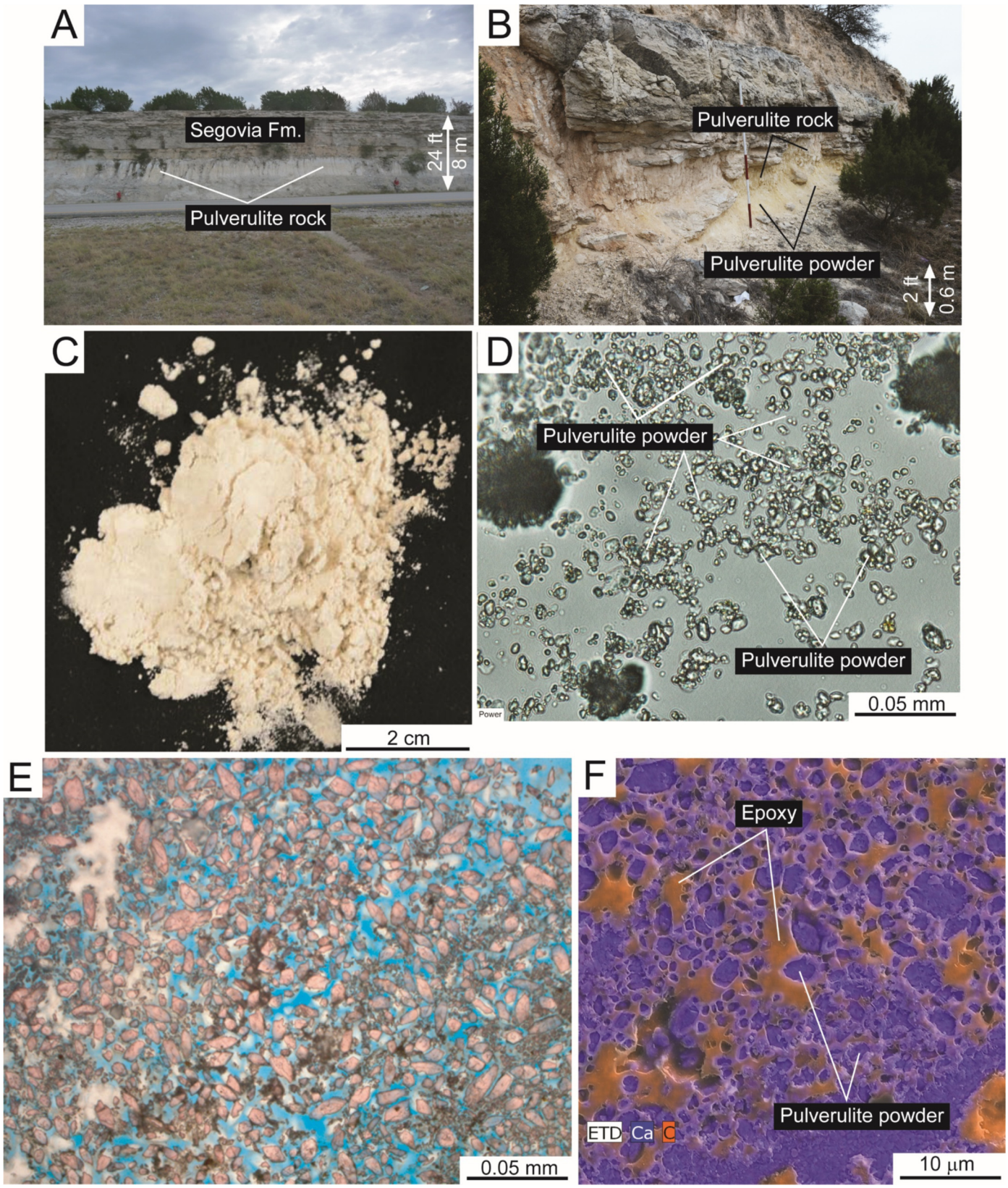

Figure 3. Pulverulite images. (A) Thick bed of pulverulite rock extending across roadcut. (B) Pulverulite rock and associated pulverulite powder. (C) Pulverulite powder. (D) Glass-slide oil mount of pulverulite powder. Particles range in size from 1 to 30 microns. (E) Thin section of pulverulite powder showing microcrystals of calcite with rounded, elongated forms. (F) SEM image of pulverulite powder overlain by energy dispersive X–ray spectroscopy (EDS) elemental map. Blue is calcite and red is epoxy. Particles have variable shapes and many are rounded.

Table 1. List of samples. See Figure 1 for location map.

Sample number	Latitude	Longitude	Sample number	Latitude	Longitude
1	N30°17.987'	W99°32.644'	21	N30°18.142'	W99°43.849'
2	N30°18.548'	W99°33.440'	22	N30°28.979'	W100°03.560'
3	N30°19.281'	W99°34.283'	23	N30°28.962'	W100°03.843'
4	N30°20.218'	W99°34.924'	24	N30°28.945'	W100°04.043'
5	N30°20.424'	W99°35.064'	25	N30°27.913'	W100°17.484'
6	N30°20.880'	W99°35.392'	26	N30°10.975'	W100°41.298'
7	N30°21.395'	W99°35.673'	27	N30°07.196'	W99°12.507'
8	N30°22.976'	W99°36.693'	28	N30°07.732'	W99°13.333'
9	N30°23.228'	W99°36.875'	29	N30°.07.834'	W99°13.543'
10	N30°24.068'	W99°.37.863'	30	N30°08.974'	W99°14.020'
11	N30°24.156'	W99°38.471'	31	N30°10.539'	W99°16.448'
12	N30°24.174'	W99°38.620'	32	N30°10.911’	W99°17.586'
13	N30°25.820'	W99°41.728'	33	N30°14.750'	W99°26.613'
14	N30°25.897'	W99°41.924'	34	N30°16.481'	W99°30.063'
15	N30°27.094'	W99°43.300'	A1–2	N30°28.415'	W99°45.072'
16	N30°27.321'	W99°43.453'	B	N30°28.380'	W99°44.813'
17	N30°28.395'	W99°44.907'	C	N30°28.011'	W99°43.796'
18	N30°28.447'	W99°45.232'	D	N30°24.016'	W99°37.986'
19	N30°28.409'	W99°45.067'	E	N30°21.555'	W99°35.805'
20	N30°28.003'	W99°43.802'	F	N30°20.980'	W99°35.457'

Selected polished thin sections showing a range of alteration intensities were viewed on a field-emission scanning electron microscope (FESEM) to characterize detailed crystal morphology, diagenetic features, and pores. A series of rock chips was viewed on the FESEM to characterize the crystals and diagenetic features in three dimensions. Ar–ion milled samples allowed fabric and texture analysis and point counting of a flat surface for porosity. An FEI Nova NanoSEM 430 system at the University of Texas at Austin was used for analysis. This FESEM equipped with in-lens secondary-electron detectors provided greatly enhanced detail of nm-scale features. Lower accelerating voltages (10 to 15 kV) were generally used on these samples to prevent beam damage, and working distances were 3 to 9 mm.

Twenty-five samples ranging from intact rock to pulverulite powder (devoid of dolomite) were selected and measured for carbon and oxygen isotopes at the Department of Geological Sciences isotope laboratory at the University of Texas at Austin. Approximately 0.3 mg aliquots were analyzed for $\delta^{13}C$ and $\delta^{18}O$ using a ThermoFisher Scientific GasBench II system coupled to a ThermoFisher Scientific MAT 253 Isotope Ratio Mass Spectrometer (Révész and Landwehr, 2002; Spötl and Vennemann, 2003). Aliquots were reacted in helium-flushed vials with 103% H_3PO_4 at 122°F (50°C) for 3 hr. Data are calibrated using calcite standards NBS–18 ($\delta^{18}O_{VPDB\ (Vienna\ Pee\ Dee\ Belemnite)}$ = -23.0‰, $\delta^{13}C_{VPDB}$ = -5.0‰) and NBS–19 ($\delta^{18}O_{VPDB}$ = -2.3‰, $\delta^{13}C_{VPDB}$ = 1.95‰). Twelve replicates of an internal carbonate standard were analyzed throughout the analytical session to account for analytical drift and precision. Analytical precision of ±0.10‰ for $\delta^{18}O_{VPDB}$ and ±0.06‰ for $\delta^{13}C_{VPDB}$ was routinely achieved.

Geographical Setting and Stratigraphy

The area of investigation (Fig. 1) is centered around Junction, Texas, in the Hill Country of the Edwards Plateau. Lower Cretaceous strata in the area are dominated by flat-lying marine carbonates of the Albian Fort Terrett and Segovia formations (Fig. 2) (Rose, 1972; Mueller, 1975). The depositional setting for these marine carbonates ranged from muddy lagoonal, to high-energy shoals, to tidal flats—some evaporitic. The initial composition of the carbonates was a mixture of calcite and Mg–calcite with lesser aragonite, as would be expected in the Lower Cretaceous greenhouse environment (Sandberg, 1983; Volery et al., 2009). At the top of the Fort Terrett Formation is the Kirschberg Evaporite Member (Fisher and Rodda, 1969; Willis et al., 2001), which was deposited in a restricted marine salina. In the area of investigation, the evaporite has been dissolved and is now a highly disturbed and brecciated zone (Fisher and Rodda, 1969). Strata in the area of investigation were probably never buried deeper than approximately1000 to 1500 ft (300 to 450 m) (Rose, 2016).

The general paleogeographic history needs to be addressed, as it may have preconditioned the strata to weather to pulverulite rock and powder. Following the deposition of Albian carbonates, a regional unconformity that separates Lower Cretaceous from Upper Cretaceous strata formed. The lower part of the Upper Cretaceous section is dominated by deeper-water marine strata such as the Buda, Eagle Ford, and Austin chalks. The upper part of the Upper Cretaceous is dominated by siliciclastics deposited in marine to subaerial environments. For a general geological history of the area, see Rose (2016).

The Edwards Plateau began to form during the Late Cretaceous while uplift related to the Laramide Orogeny started in West Texas and subsidence initiated in the ancestral Gulf of Mexico in the east (Ewing, 1991; Barker et al., 1994). Related to the uplift of the Edwards Plateau, Upper Cretaceous and overlying strata were eroded (Adkins, 1933; Kastning, 1981; Barker et al., 1994). In the Junction area, the Albian strata are now exposed. Their exposure history dates back to at least the Miocene, if not much earlier (Caber, 2010). During millions of years of exposure, Upper Cretaceous strata were eroded and Lower Cretaceous carbonate strata were highly karsted (Kastning, 1981, 1984). Also during this long history of exposure, the Kirschberg Evaporite Member dissolved in some areas; overlying strata

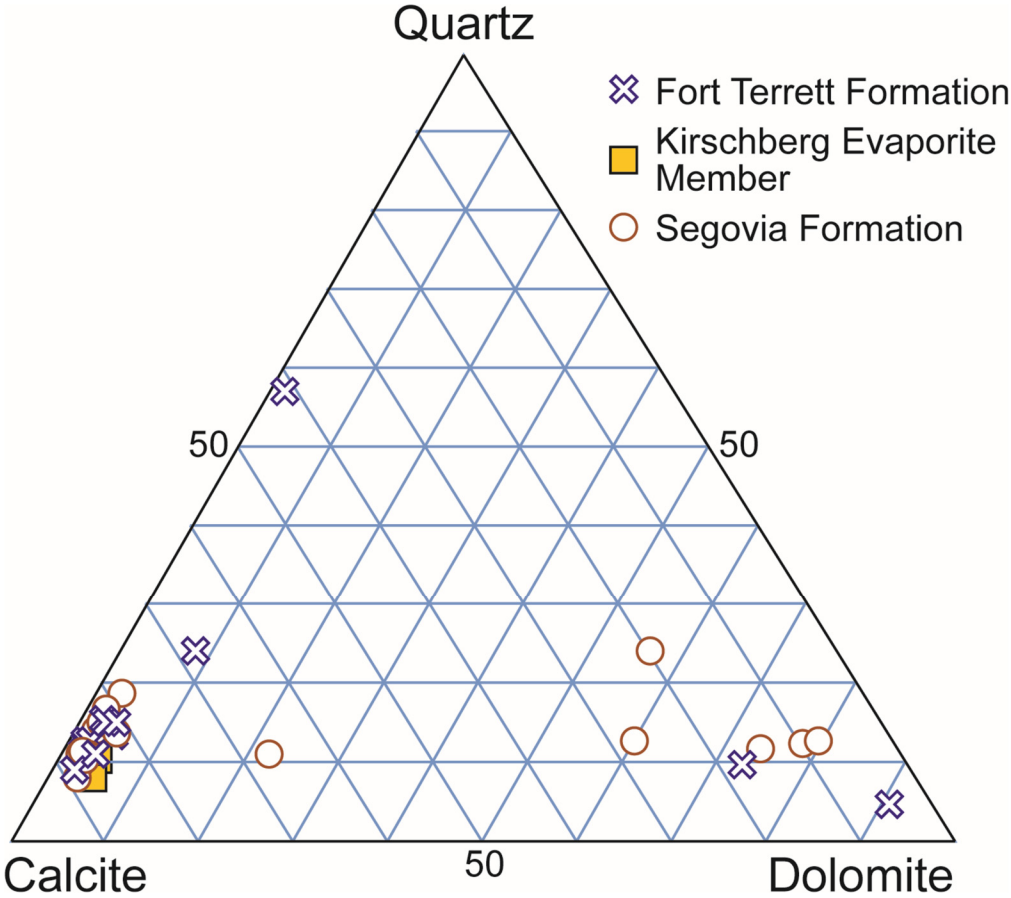

Figure 4. XRD mineralogic analyses of pulverulite powder. Powder shows two populations: one of a limestone precursor and one of a dolostone precursor.

collapsed and resulting breccias were lithified (Fisher and Rodda, 1969; Rose, 1972; Mueller, 1975).

Carbonate strata on the plateau host the Edwards-Trinity Aquifer (Hopkins, 1995). The groundwater table has fluctuated many times during the Edwards Plateau history, and formation of caves is common (Kastning, 1981, 1983; Ferrill et al., 2004; Caber, 2010). In the area of investigation, the strata are well above the present water table.

Because part of this investigation relates to recent weathering, recent climatic data are relevant. According to U.S. Climate Data (2017), the average annual temperature for the Junction area is 64.2°F (17.9°C) (average low is 48.5°F [9.2°C] and average high is 79.8°F [26.6°C]). June, July, and August are the hottest months and December, January, and February are the coldest months. Average temperature lows in December and January are below freezing. Snowfall averages 1 in (2.54 cm) per yr. Average annual precipitation is 24.6 in (62.5 cm).

CHARACTERIZATION OF PULVERULITE

Introduction to the Term *Pulverulite*

The term *pulverulent* means "fine powder" and is a derivative of the Latin word *pulverulentus* (dusty) (Merriam-Webster Dictionary, 2017). Shumard (1886) first used the term *pulverulite* to refer to a limestone with the consistency of pulverized chalk (probably pulverulite rock). As mentioned earlier, pulverulite rock and powder in the Junction area (Fig. 3) can be dominated by calcite or dolomite (Rose, 1972; Mueller, 1975). Most of the samples collected and emphasized in this investigation are dominated by limestone to dolomitic limestone (Fig. 4), although some dolomite-dominated samples were also analyzed.

Pulverulite, with or without differentiation into rock and powder, has been mentioned a number of times in the literature. The two main origins of pulverulite are associated with sedimentary rocks (e.g., Shumard, 1886; Blank and Tynes, 1965; Chafetz and Butler, 1980; Kolb, 1981; Jones et al., 1989; Mahler et al., 1999; Hauwert, 2009; Kahle, 2012; Poros et al., 2013) and with volcanic rocks (e.g., Richards and Bryan, 1933; Blank, 1965; Martin and Malahoff, 1965). Pulverulite associated with sedimentary rocks is generally thought to be a weathering-alteration product (Fig. 5) (e.g., Rose 1972) related to dissolution and in some cases reprecipitation (caliche) (Blank and Tynes, 1965); Poros et al. (2013) concluded that in Triassic dolostones in the Buda Hills, Hungary, the powderization was associated with cryogenic processes. Most of the pulverulite examples in the literature are dolomite dominated (e.g., Chafetz and Butler, 1980; Jones et al., 1989; Hauwert, 2009; Kahle, 2012; Poros et al., 2013).

Several occurrences of pulverulized carbonates are also known from the subsurface, where laterally extensive pulverulitic zones are attributed to former subaerial exposure (regional karstic) events (e.g., Fu et al., 2004; Ji et al., 2004; Machel et al., 2012) and preserved during subsequent burial events. A few smaller pulverulite bodies, in the close vicinity of structural elements, are interpreted to have been formed in the subsurface (e.g., Dewever, 2008).

Description of Pulverulite in the Junction Area

Pulverulite rock and powder occur in both the Fort Terrett and Segovia formations (Figs. 2 and 6) in the area of investigation, usually in microporous skeletal peloidal wackestones and packstones (Figs. 7A, 8A, and 9A). Most pulverulite rock and powder follow the original horizontal bedding (Fig. 3A), but

some form pods or lenses and subvertical pipes. Hauwert (2009) noted that pulverulitic rock beds within the Kirschberg Member are visible in the walls of caves and in downhole videos of wells in the Central Texas area. Cavers have also noted pulverulite powder on walls in Central Texas caves. The senior author recognized transported pulverulite powder in Tertiary-aged paleocaves along Interstate 10 in the Sonora area.

Pulverulite rock strata generally extend along the length of roadcuts (hundreds of feet) (Fig. 3A), but sometimes pinch out into less-weathered strata in one or both directions. Pulverulite powder associated with these pulverulitic strata occurs where a lower recessive ledge formed (Fig. 3B). Excavating back into the powder exposes firmer pulverulite rock.

The mineralogy of pulverulite rock and powder in the area of investigation is mainly calcite, but some samples are dominated by dolomite (Fig. 4). Pulverulite appears to be a product of limestone or very dolomitic limestone (Mueller, 1975). Calcite-dominated samples have up to 22% quartz and generally less than 6% dolomite, as determined by XRD analysis performed by the Bureau of Economic Geology laboratory. Dolomite-dominated samples also contain up to 22% quartz and up to 30% calcite. In the parent rock, some of the dolomite rhombs are well zoned, and a few show minor dissolution of their cores (Fig. 7C and 7D). In the slightly weathered dolomite-bearing rock, centers of the zoned dolomite are dissolved (Figs. 7B and 8C). In other pulverulite rock, dolomite crystals are totally dissolved, leaving rhombic-shaped molds (Figs. 9A and 9B).

Particles in pulverulite rock and powder range widely in size, generally between 1 and 10 µm (Figs. 3 and 9). Some microcrystals may be up to 50 µm, but others can also be less than a micron. Size distribution of the particles is generally very poorly to poorly sorted, but some are moderately sorted. In pulverulite rock, crystals show light cementation, as indicated by interlocking crystals (Fig. 9C), which are the result of competitive cementation among crystals competing for space. Rare fossils—more-robust shells such as oysters and echinoderm fragments—are preserved in the pulverulite rock (Fig. 9A). Remnants of peloids are present as clusters of microrhombic calcite (Fig. 8B). Some of these characteristics were also noted by other authors who studied this area (e.g., Rose, 1972; Mueller, 1975). However, none of the earlier researchers suggested that pulverulite rock or powder were products of microcrystalline and microporous carbonate mud-rich strata, nor did they identify the stages of formation.

Paragenesis of Pulverulite Rock and Powder

The transition from relatively-unaltered parent rock to pulverulite rock to pulverulite powder is a relatively simple process (Figs. 5 and 6). The most important factor for the formation of pulverulite types investigated in the Junction area is the lithology of the parent rock, notably the presence of very porous microcrystalline limestone to dolomitic limestone (occasionally dolostones) (Fig. 7). The stages of pulverulite rock and powder formation are shown in Figures 5 and 6 and described in the following subsections.

Relatively-Unaltered Parent Rock (Figs. 5–7)

The lithology of the relatively-unaltered parent rock, a fine-grained and microporous limestone, is the main controlling factor for the formation of pulverulite rock and powder. Strata in the Fort Terrett and Segovia formations in the Junction area were deposited on a broad, shallow-water platform 100 mi (160 km) behind the Stuart City reef trend to the south (Fisher and Rodda, 1969). The depositional environments ranged from low-energy

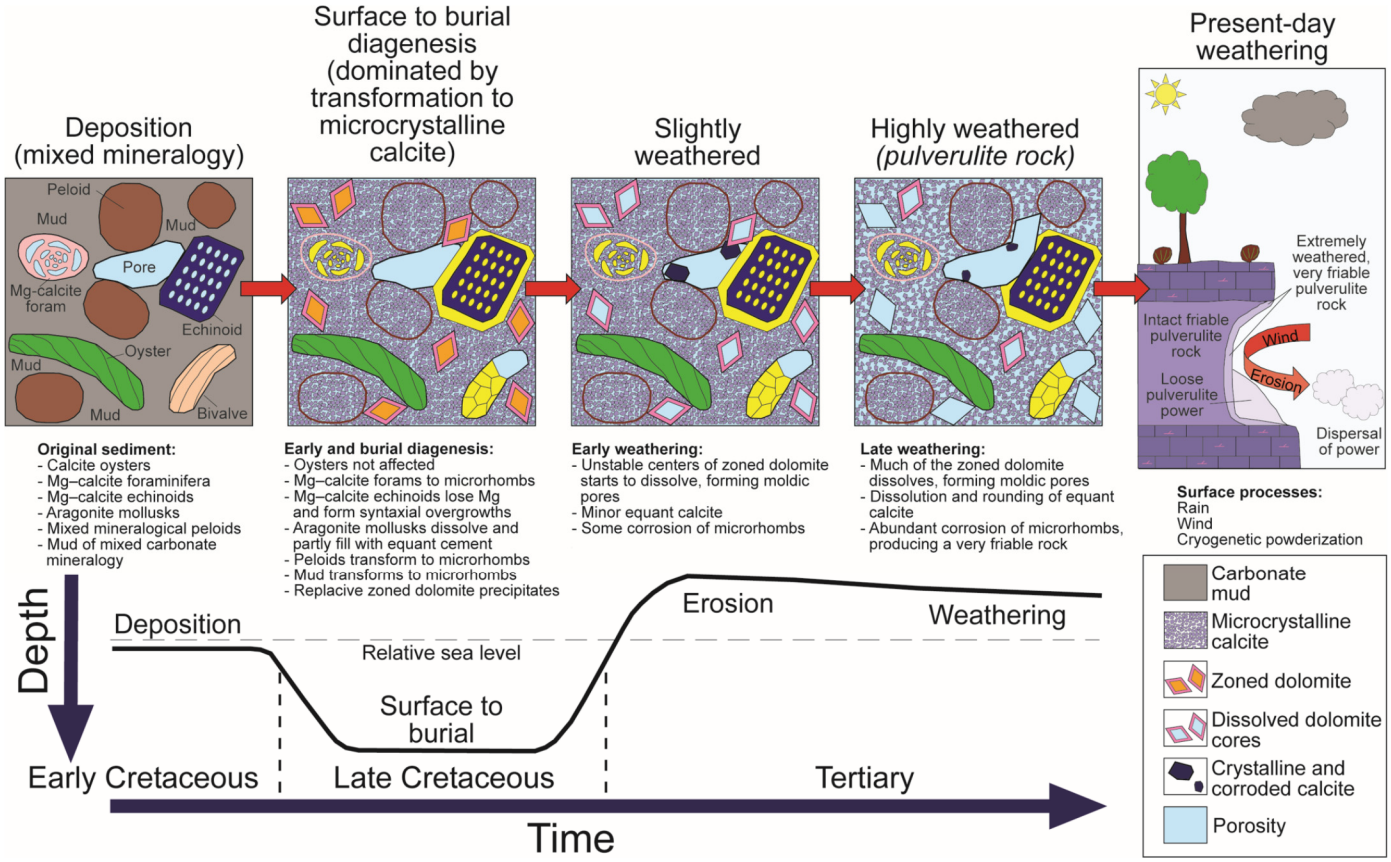

Figure 5. Schematic illustrating stages of diagenesis. The relative burial-history curve is also presented.

subtidal to moderate- to high-energy shoaling conditions in some areas. The lime-mud-rich, low-energy carbonates are considered to have been composed of a mud mixture of calcite and Mg–calcite with lesser amounts of aragonite. This original mud mixture is postulated on the concept that the Lower Cretaceous Albian section was deposited during a Greenhouse time that favored lime mud of this composition (Sandberg, 1983; Volery et al., 2009). This composition of lime mud can produce very microporous lime wackestones and packstones upon early meteoric to shallow-burial diagenesis (e.g., Volery et al., 2009; Volery, 2010; Loucks et al., 2013; Lucia and Loucks, 2013; Kaczmarek et al., 2015), as is well documented in the Middle East (e.g., Volery et al., 2009) (Fig. 10). Some of these Middle East limestones have porosities up to 40%. The Junction area microporous wackestones and packstones have similar reservoir quality. Based on point counts of six samples, the parent limestone rock has ~17% porosity; when slightly altered, it has ~28% porosity, and the resulting pulverulite rock has 46% porosity.

As the mud-matrix-rich sediments transformed to lime wackestones and packstones, the muds converted to a very porous microcrystalline texture (Figs. 6 and 7). Crystal size is variable (generally less than 10 μm) and the crystals are moderately well cemented (Figs. 6 and 7). Some initial dissolution of the microcrystals is noted. Some coarser dolomite cement is present, incorporating mud-sized calcite crystals at its boundary (Fig. 7F). Rare fossil fragments are preserved (Fig. 7D). According to Mueller (1975), some of these limestones were partly dolomitized early in their history. Few of the limestones were completely dolomitized. Dolomite crystal sizes generally range between 40 and 50 μm. Some dolomite is well zoned (Fig. 7C and 7D) and displays dissolution that started in the crystal centers (Fig. 7B). In effect, this type of parent rock is a microporous dolomitic limestone consisting of a porous microcrystalline calcite matrix between dolomite crystals (Fig. 7B). An equant, nonluminescent calcite cement phase—precipitated in macrointerparticle and macrointraparticle pores—postdates replacive dolomite formation but predates dissolution of dolomite crystal cores (Fig. 8A). Calcite crystals, like dolomite rhombs, are commonly corroded, resulting in the rounded shape of many crystals. Minor amounts of clay are present and apparently encased in calcite crystals (Fig. 8E).

Slightly- to Moderately-Altered Parent Rock (Figs. 5, 6, and 8)

Early weathering affected microcrystalline calcite crystals, equant calcite cement, and dolomite rhombs. The microcrystalline calcite underwent some dissolution, as indicated by etched and pitted surfaces as well as dissolution between crystals (Fig. 8). Remnant crystal facies are preserved. This stage of diagenesis produced a more porous rock texture through dissolution (Fig. 8), which also dissolved cement, allowing the rock to become more friable.

Some samples contain nanocrystals of calcite (e.g., Fig. 9F) ranging in size from 500 to 1000 nm, which appear to be on the surface of much larger crystals (Fig. 9F; tens of microns). These nanocrystals—which contributed to the pulverulite powder—are possibly the product of weathering, where the larger microcrystals underwent dissolution and thus provided the calcium carbonate for the nanocrystals.

The zoned dolomite crystals display dissolved dolomite cores (Fig. 8C). Such textures generally are the product of dissolution of more-soluble crystal cores relative to more-stable dolomitic outer rims. The rock remains relatively intact if the dolomite forms a rigid interconnected framework; the hollow centers of the dolomite crystals do not significantly affect the rock's mechanical stability (e.g., Fig. 7B).

Intensely-Altered Parent Rock (Pulverulite Rock) (Figs. 5, 6, and 9)

At an advanced stage of alteration, the rock becomes very friable and can be disaggregated by hand. The microcrystalline

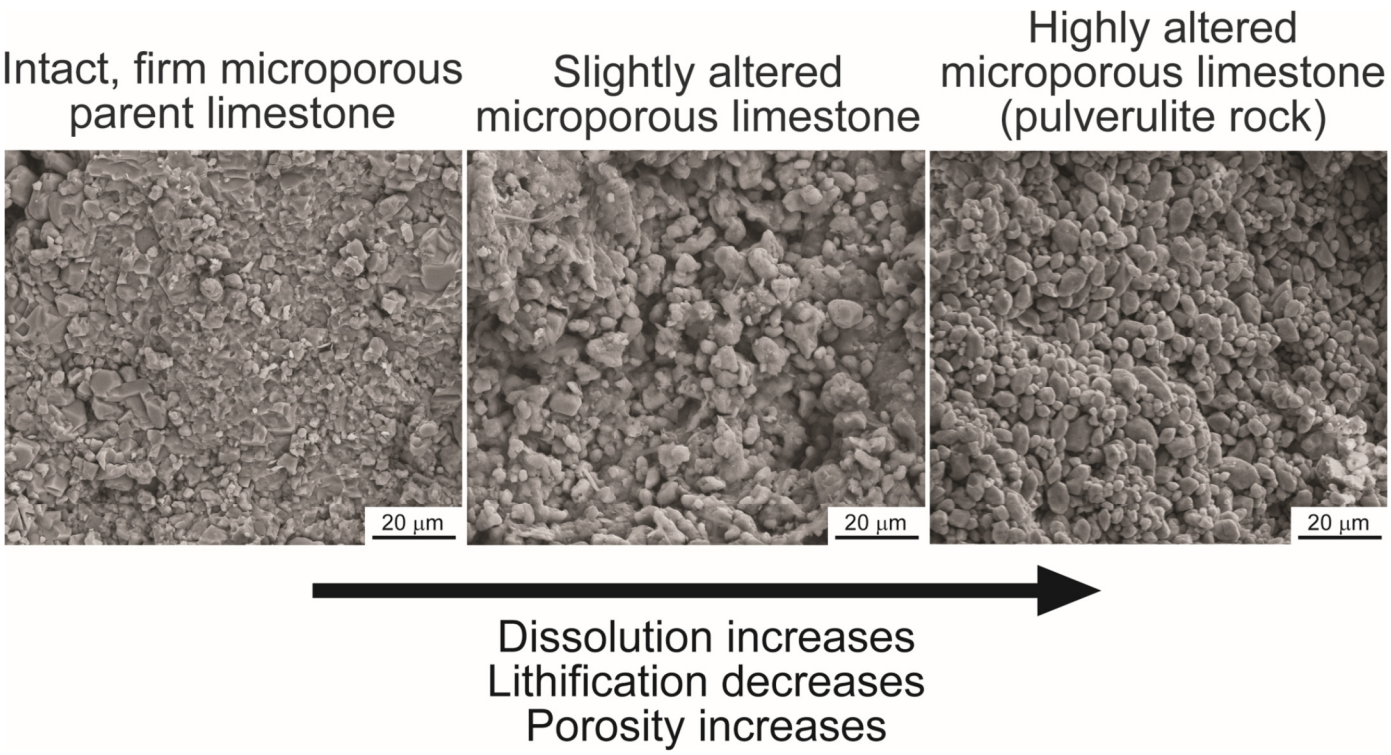

Figure 6. SEM images showing the transition from intact-host microporous parent limestone to slightly-altered limestone to very-altered limestone (pulverulite rock).

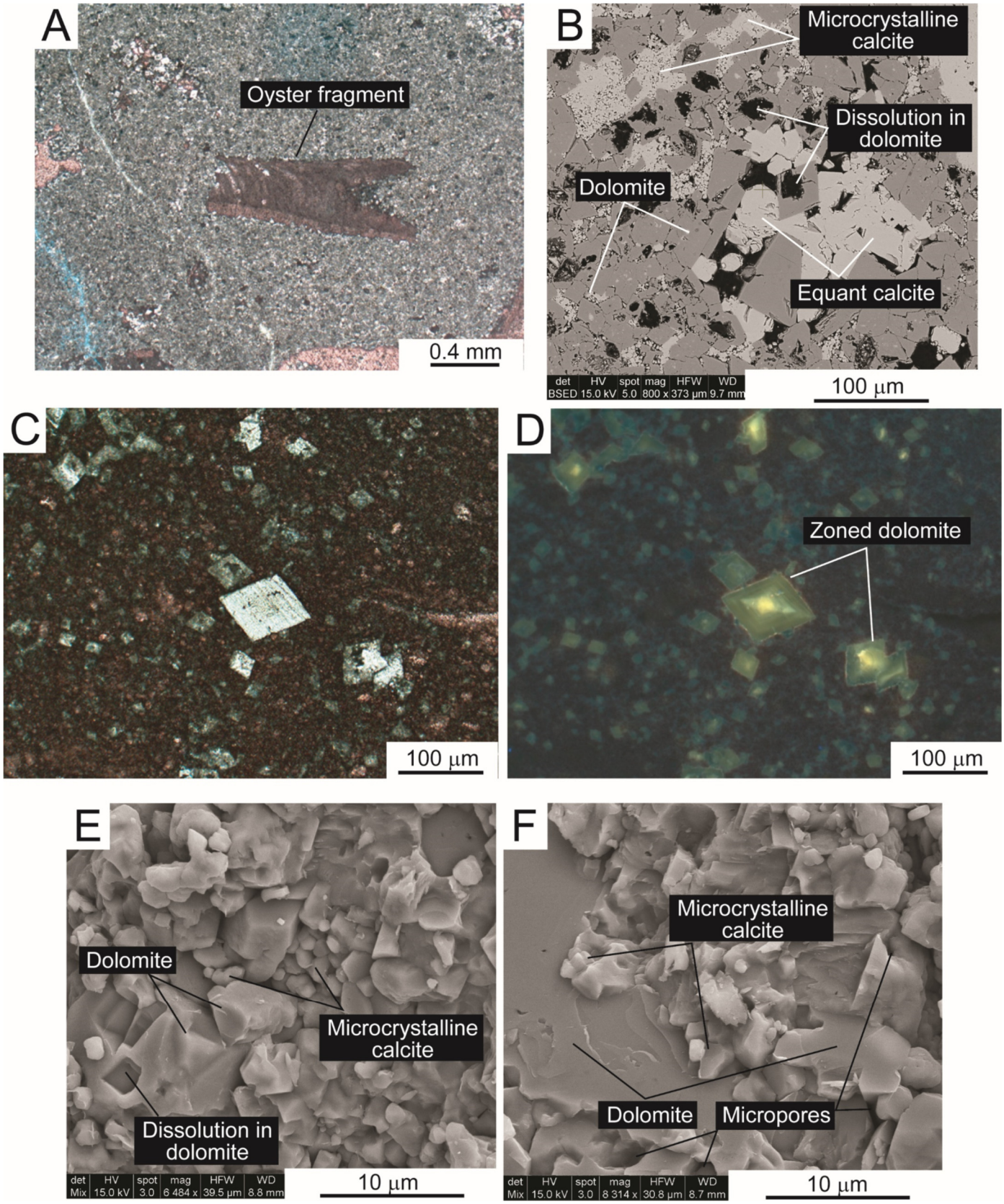

Figure 7. Intact host rock. (A) Microporous skeletal peloidal wackestone containing oyster fragment. (B) Backscattered SEM image. The microcrystalline calcite is light shaded and the dolomite is dark shaded. In this sample, the dolomite forms the rigid framework. Some dolomite cores show dissolution. (C) Zoned dolomite crystals in peloidal packstone. (D) Zoned dolomite crystals under UV light. Same area as C. (E) SEM image of rock chip. The crystals and particles are well cemented and display well-developed crystal facies. Some micropores are present. (F) SEM image of rock chip. Dolomite has incorporated microcrystalline calcite at its edge.

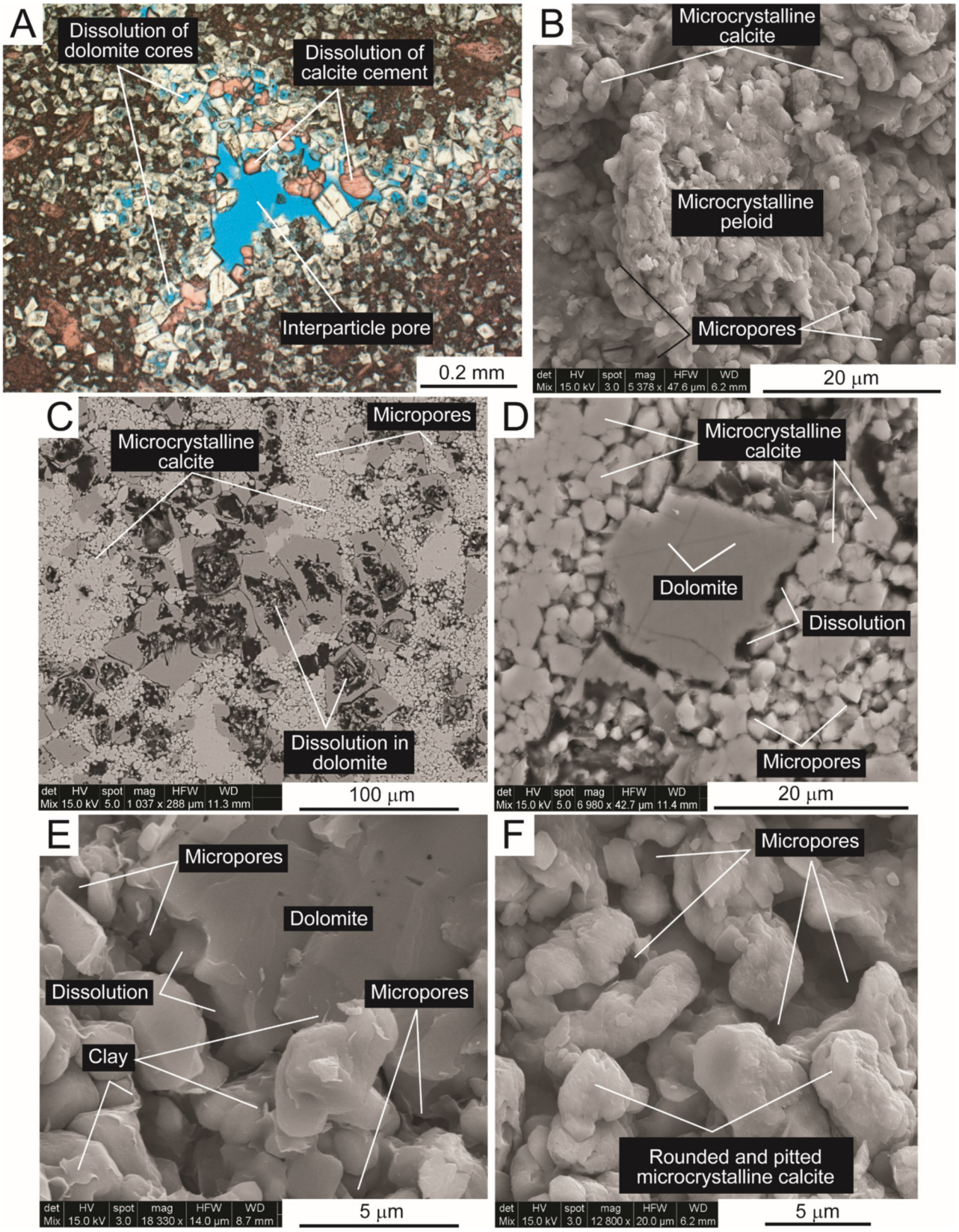

Figure 8. Slightly-weathered host rock. (A) Microporous peloidal wackestone showing dissolution (rounding of edges) of equant calcite (stained red) and dolomite crystal cores (stained blue). (B) SEM image of rock chip. Peloid composed of microcrystals. Matrix shows solution of microcrystals and presence of micropores. (C) Back-scattered SEM image. The calcite is light shaded and the dolomite is dark shaded. The microcrystalline calcite is very microporous. The centers of the dolomite crystals show strong dissolution. (D) Ar–ion-milled SEM image of slightly-rounded microcrystalline calcite with micropores and a crystal of dolomite showing grain-edge dissolution. (E) SEM image of rock chip. Microcrystalline calcite is cemented but porous and displays some clay flakes. The dolomite shows grain-edge dissolution. (F) SEM image of rock chip. The microcrystalline calcite shows strong pitting of the surface. Crystals are very irregular in shape.

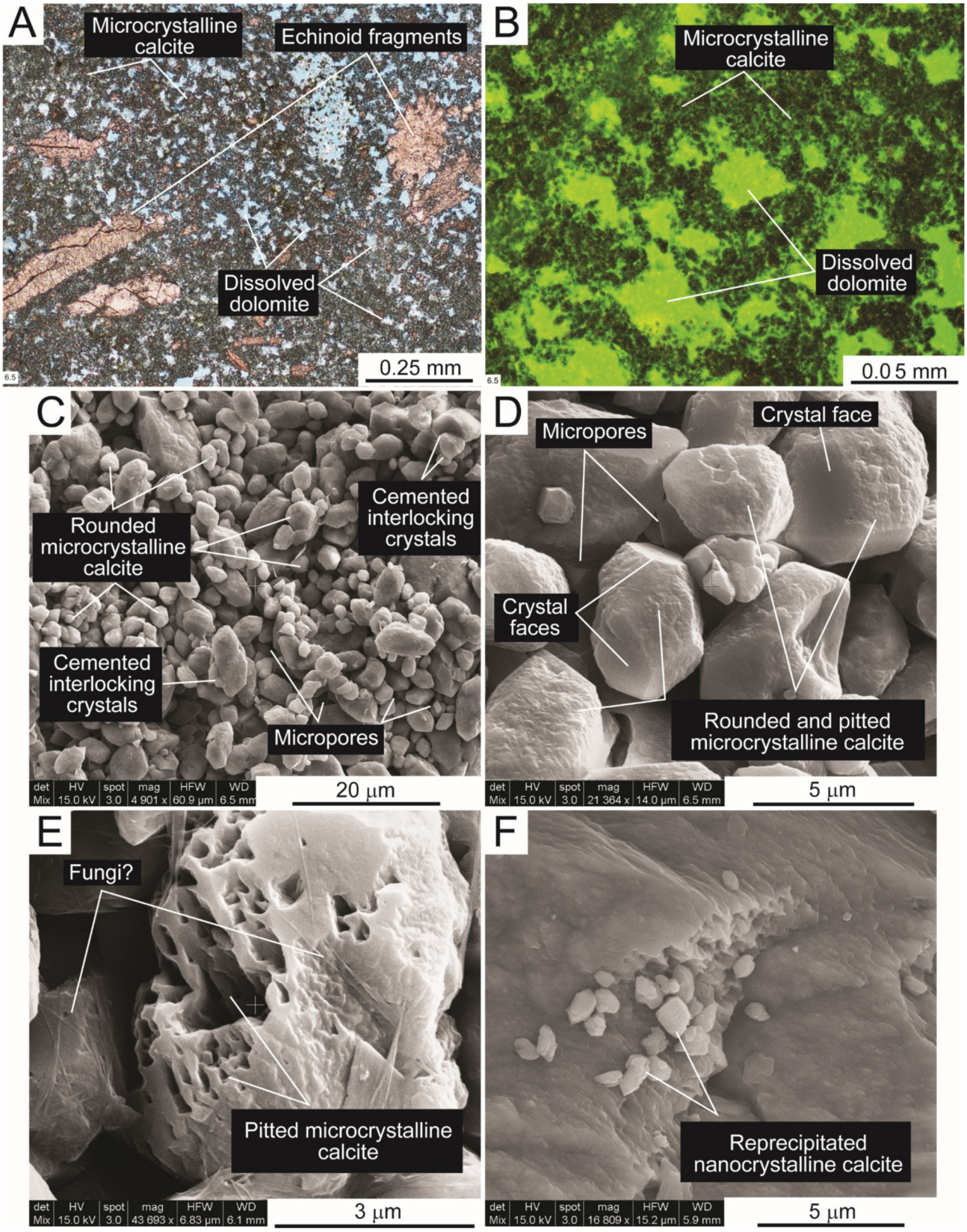

Figure 9. Very-weathered host rock (pulverulite rock). (A) Very-weathered, microporous, skeletal peloidal wackestone containing echinoid fragments. The former dolomite is now moldic pores. (B) Thin-section photomicrograph of pulverulite powder in green UV light. Bright green is pore space. The microcrystalline calcite is very-weakly cemented. The dissolved dolomite forms moldic pores. (C) SEM image of rock chip. The nearly-loose microcrystalline calcite shows well-developed rounding and pitting. (D) SEM image of rock chip. Close-up of microcrystalline calcite. No cementation is apparent, and the crystals are well rounded and pitted. Some crystal faces are preserved. (E) SEM image of rock chip. Microcrystal of calcite shows strong dissolution. The fine threads may be fungi. (F) SEM image of rock chip. Nanocrystals of calcite may be a product of dissolution and reprecipitation in the weathering zone.

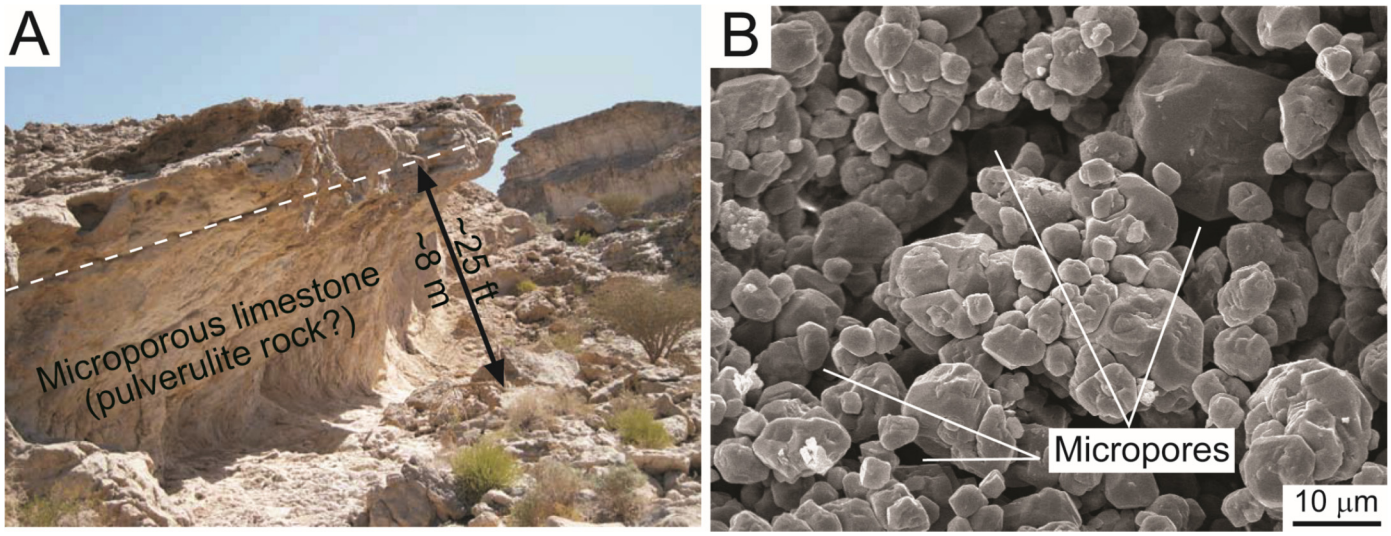

Figure 10. Examples of Middle East microporous limestones. (A) Outcrop of a microporous limestone from the Natih Formation (Cenomanian to early Turonian) in Oman. Notice that at this outcrop, the pulverulite power appears to have been dispersed. (B) SEM image of rock chip. Sample is from the Mishrif Formation (Cenomanian to early Turonian) in Qatar (4675 ft [1425 m]). Microporous limestones, such as seen in this sample, are common reservoirs in the Middle East. Both photographs are reproduced with the permission of Chadia Volery (left: Volery [2010]; right: Volery et al. [2009]).

calcite is much more rounded (Figs. 6, 9C, and 9D) by dissolution than the microcrystals noted in earlier stages of alteration. Surfaces of the crystals are densely pitted (Fig. 9D and 9E). Very little cement remains, and the grains are attached only at grain contacts (Fig. 9C). Porosity is higher, presently ~46% as compared to ~17% in the unaltered parent rock. Some of the original grains that transformed to microcrystalline calcite are still recognizable (Fig. 9A). In some samples, the dolomite rhombs are totally dissolved, leaving rhombic-shaped moldic pores (Fig. 9A and 9B).

Pulverulite Powder (Figs. 3 and 5)

The powder is basically the final breakdown of very porous and friable pulverulite rock. Calcite powder, nearly devoid of dolomite, is commonly associated with the limestone parent rock or with the slightly dolomitic parent limestone. Dolomite powders are likely to form from a dolomite-rich parent rock but not necessarily pure dolostone (Mueller, 1975).

Stable Isotope Data

The stable isotopic compositions of bulk samples, containing only a calcite phase, were measured from all stages of alteration. The data form a commonly observed distribution typical for meteoric diagenesis (Lohmann, 1988), with negative oxygen and negative carbon isotope values, whereby the carbon isotope values display a much larger range (Fig. 11). The $\delta^{18}O$ composition ranges from -4.7 to -3.7‰ for most of the data. The parent rock is less negative in $\delta^{13}C$ composition (~0 to -4‰) compared to the powder samples (~-1 to -7.5‰). The isotopic composition of the pulverulite rock samples falls between the unaltered rock and the powder samples, representing a transitional stage of disintegration from parent rock to loose powder.

DISCUSSION

Origin of Pulverulite Rock and Powder

Stable isotopic data show that the alteration of the parent rock to pulverulite rock and powder happens in the meteoric diagenetic realm, which supports our interpretation that disintegration of the investigated carbonate rock is a subaerial, exposure-related weathering process; our findings certainly fit with other observations that the pulverulite powder is related to exposure to an open environment such as a roadcut (Rose, 1972; Mueller, 1975) or a cave passage (Mahler et al., 1999). As noted earlier, the powder appears within a few years of the excavation of a roadcut.

Pulverulite rock is a product of microporous limestones and microporous dolomitic limestones in the zone of weathering, as noted by the dissolution, pitting, and rounding of intertidal microcrystals. The gradation along bedding from relatively unaltered microporous parent rock to highly altered pulverulite rock also supports the concept that microporous rocks can weather to pulverulite rock and powder.

The simplest processes for producing breakdown to powder are the dissolution of the last of the calcite cement that barely holds the rock together or the mechanical impact of rain drops against friable rock. Another possibility is cryogenic powderization (Poros et al., 2013). As recorded by U.S. Climate Data (2017), average temperature lows in December and January at Junction are below freezing, and freeze/thaw cycles could be produced within the rock face.

At least one additional factor could have aided the formation of pulverulite rock and powder at Junction: the force of calcite crystallization in the parent rock, driven either by cycles of wetting and drying in the wet months of the year, or by localized reprecipitation of the carbonate that was dissolved "upstream" (i.e., near the entry points or areas of rain water). Mineral expansion driven by wetting-drying cycles is a nearly ubiquitous process recognized worldwide in the weathering of all sorts of rocks, perhaps best known from the weathering of buildings, monuments, and statues (e.g., Siegesmund and Snethlage, 2011). In the studied strata, newly formed calcite crystals are not uncommon; however, we have little petrographic evidence for the process, but the possibility of this crystallization being a contributing factor to pulverization cannot be ruled out. The stable isotope data of the calcite samples—indicating precipitation of calcite in the meteoric zone—are consistent with this alternative. Also, Willis et al. (2001) documented many examples of calcification within the Edwards strata in the Junction area.

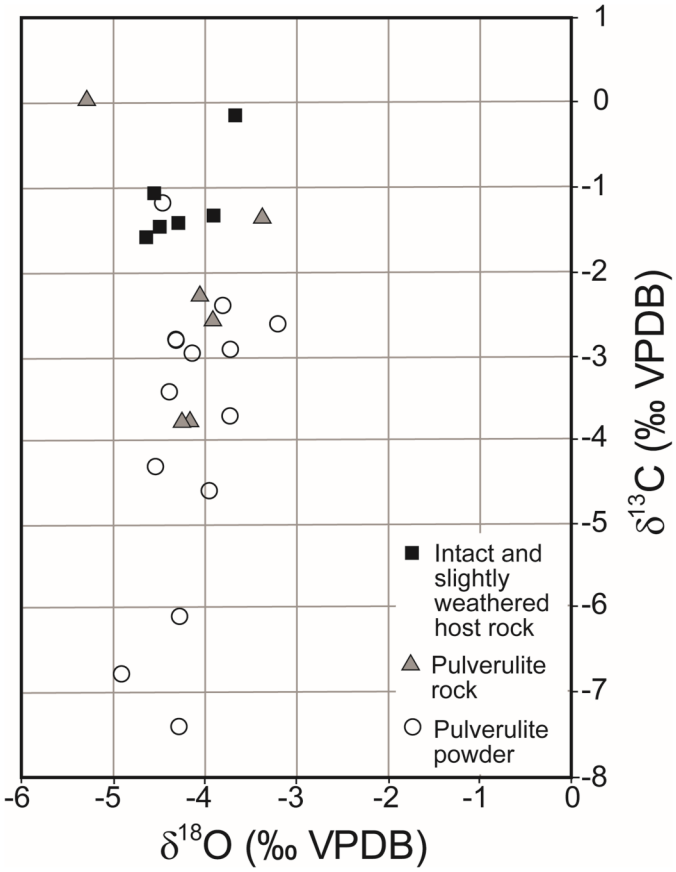

Figure 11. Carbon and oxygen isotope plot of calcite samples. Samples range from intact parent rock to pulverulite powder.

The surprising thing about the pulverulite powder is that it is not blown away, despite being so lightweight. Photographs of similar microporous rocks in the Middle East show a thick microporous bed (pulverulite rock?) eroding back, but not exhibiting abundant, if any, pulverulite powder at its base (Fig. 10A). The difference between the two areas (Junction and Oman) may be that the Middle East climate is dry enough to keep the powder sufficiently loose to be dispersed by the wind, whereas the moister climate of the Junction area makes erosion of the powder by the wind more difficult. However, it needs to be noted that researchers of this investigation did no fieldwork in the Middle East and that pulverulite powder may be present in other areas.

Pulverulite Rock- and Powder-Related Hydrocarbon Reservoirs

The intense alteration (weathering) of microporous limestones such as seen in the Junction area and in the Middle East (Fig. 10) (e.g., Volery et al., 2009) can produce a pulverulitic rock that may be preserved into the ancient record. This highly altered rock texture would be an indication of subaerial or near-subaerial exposure (in an active groundwater aquifer). Deville de Periere et al. (2011), in a study of microporous limestones in the Middle East, classified porous micrites (microcrystalline particles) into four classes based on particle morphology. Their class of microcrystalline particles that are rounded and very lightly cemented at grain contacts appears very similar to the rounded microcrystalline particles in the Junction pulverulite rock (Figs. 6 and 9). Deville de Periere et al. (2011) speculated that these Middle East microporous limestones may be the product, in part, of weathering at some point in their history. Deville de Periere et al. (2011) reported that some of these microporous rocks are associated with major exposure surfaces and are very porous (>30% porosity).

An example (proprietary study; therefore, no name or location can be provided) of relict pulverulite powder was noted in a lower Paleozoic, slightly dolomitic limestone at the top of a very porous weathered zone just beneath an unconformity (Fig. 12). Above the unconformity is a tight-sealing siliceous mudstone. The pulverulite powder is now well cemented but still porous (Fig. 12C–E), containing broken and weathered clasts of chert surrounded by patina rinds produced by weathering. The pulverulite powder shows a high degree of disruption by root mottling (Fig. 12A and 12B). Thin sections contain weathered relict calcite allochems and small root traces (Fig. 12B). Abundant micropores in the relict pulverulite powder are evident from viewing blue-fluorescent-dyed thin sections with UV light under a petrographic microscope (Fig. 12C). Ar–ion milled samples of the cemented pulverulite powder viewed under the SEM show interparticle pores that range in size from >1 to 10 µm (Fig. 12D and 12E) and have an intercrystalline shape, suggesting that the weathered particles acted as nuclei for calcite overgrowths (Fig. 12E).

Therefore, pulverulite rock with rounded and pitted (possibly obscured by cementation) microcrystals can be an important criterion for recognizing major exposure surfaces in microporous limestones. Pulverulite rock and associated weathered rocks, because of their enhanced porosity compared to the unweathered parent rock, may be potential microporous reservoirs.

CONCLUSIONS

Pulverulite rock and powder are weathering products of microporous limestones and microporous dolomitic limestones (and occasionally dolostones) in the Central Texas area. Similar rocks appear in the Middle East. Pulverulite rock where still lightly cemented forms friable pulverulitic strata; where it breaks down into individual particles or microcrystals, it forms pulverulite powder. In the Central Texas area, the transition from intact, firm, microporous parent rock to pulverulite powder was well documented. As weathering of the microcrystals proceeds, they become more rounded and pitted, and the mount of cement binding the microcrystals decreases.

The transition from pulverulite rock to powder occurs where the rock is exposed to the open air—e.g., along a roadcut, an outcrop, or a large solution opening such as a cave. The production of pulverulite powder is very rapid (tens of years) and may be the product of the last stage of dissolution, or of mechanical processes such as raindrop impact, cryogenic powderization associated with freeze/thaw cycles, or the force of recent crystallization of calcite from dissolved carbonate in the weathering zone.

Pulverulite rock and relict powder are important to recognize in the ancient record because they are evidence of subaerial weathering. These rocks may form reservoir-quality strata beneath unconformities.

ACKNOWLEDGMENTS

This study was funded by the Carbonate Reservoir Characterization Research Laboratory (RCRL) at the Bureau of Economic Geology (Bureau), University of Texas at Austin. We thank all of the RCRL sponsors for their support. Patrick Smith of the Bureau helped with the SEM images, and Harry Rowe, formerly of the Bureau, analyzed XRD powders. Aimee Villarreal of ConocoPhillips helped the authors complete the initial fieldwork. Chadia Volery of Royal Dutch Shell kindly provided permission to use several photographs from her publications. Stephanie Jones of the Bureau edited the initial manuscript. David Hull, James Willis, and an anonymous individual reviewed the manuscript and provided valuable feedback and suggestions

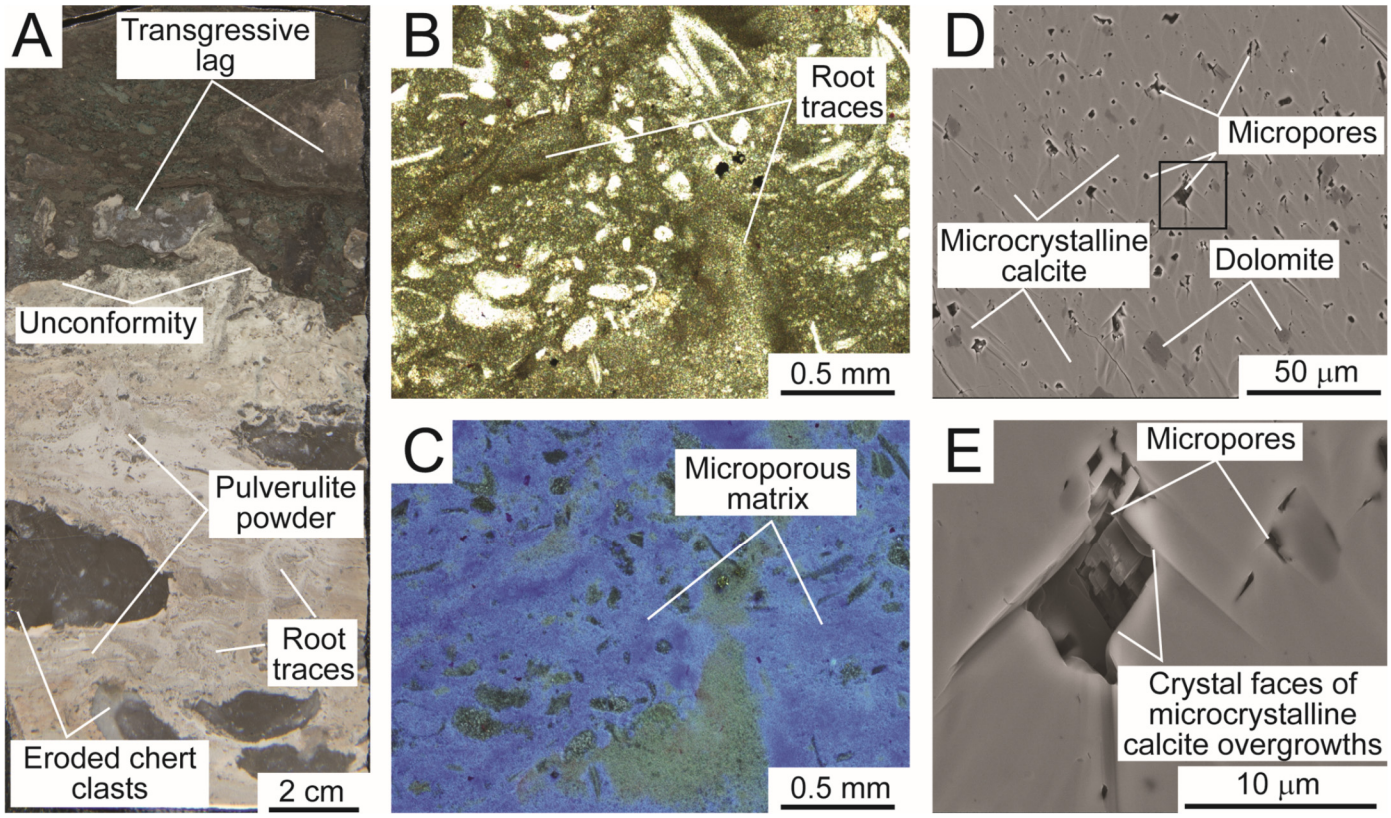

Figure 12. Ancient, lower Paleozoic, relict pulverulite powder. (A) Core slab. Lithified pulverulite powder in an exposure surface directly under a major unconformity. The relict pulverulite powder contains broken chert clasts and root traces. (B) Thin section of the relict pulverulite showing root traces. (C) Same as B but under blue UV light. The blue areas are microporous. (D) Ar–ion milled SEM image. Rhombic-shaped micropores are the result of calcite overgrowths on the microcrystals in the relict powder. (E) Close-up of boxed area shown in D. The crystal faces of calcite overgrowths on the relict pulverulite particles are displayed. The intercrystalline pores are in the nano- to micron-size range. No identification information can be provided for this case history because it is from a proprietary study; however, permission was granted to provide these images.

for improvement. Publication authorized by the Director, Bureau of Economic Geology, Jackson School of Geosciences, University of Texas at Austin.

REFERENCES CITED

Adkins, W. S., 1933, The Mesozoic systems in Texas, *in* E. H. Sellards, W. S. Adkins, and F. B. Plummer, eds., The geology of Texas, v. I, stratigraphy: University of Texas Bulletin 3232, Austin, p. 239–518, <https://repositories.lib.utexas.edu/handle/2152/24040> Last accessed August 27, 2018.

Barker, R. A., P. W. Bush, and E. T. Barker, 1994, Geologic history and hydrogeologic setting of the Edwards-Trinity Aquifer System, west-central Texas: U.S. Geological Survey Water-Resources Investigations Report 94–4039, 51 p., <https://pubs.er.usgs.gov/publication/wri944039> Last accessed August 27, 2018.

Blank, H. R., Jr., 1965, Ash-flow deposits of the central King Country, New Zealand: New Zealand Journal of Geology and Geophysics, v. 8, p. 588–610, doi:10.1080/00288306.1965.10423193.

Blank, H. R., Jr., and E. W. Tynes, 1965, Formation of caliche in situ: Geological Society of America Bulletin, v. 76, p. 1387–1392, doi:10.1130/0016-7606(1965)76[1387:FOCIS]2.0.CO;2.

Caber, R. H., 2010, Paleocaves and associated features in the Lower Cretaceous Segovia Formation, western Edwards Plateau, West Texas: M.S. Thesis, University of Texas at Austin, 164 p.

Chafetz, H. S., and J. C. Butler, 1980, Petrology of recent caliche, pisolites, and speleothem deposits from Central Texas: Sedimentology, v. 27, p. 497–518, doi:10.1111/j.1365-3091.1980.tb01644.x.

Deville de Periere, M., C. Durlet, E. Vennin, L. Lambert, R. Bourillot, B. Caline, and E. Poli, 2011, Morphometry of micrite particles in Cretaceous microporous limestones of the Middle East: Influence on reservoir properties: Marine and Petroleum Geology, v. 28, p. 1727–1750, doi:10.1016/j.marpetgeo.2011.05.002.

Dewever, B., 2008, Diagenesis and fluid flow in the Sicilian fold-and-thrust belt: Ph.D. Dissertation, *Katholieke Universiteit Leuven*, Flanders, Belgium, 184 p.

Ewing, T. E., 1991, The tectonic framework of Texas, with accompanying tectonic map of Texas: Bureau of Economic Geology, Austin, Texas, 36 p.

Ferrill, D. A., D. W. Sims, D. J. Waiting, A. P. Morris, N. M. Franklin, and A. L. Schultz, 2004, Structural framework of the Edwards Aquifer recharge zone in south-central Texas: Geological Society of America Bulletin, v. 116, p. 407–418, doi:10.1130/B25174.1.

Fisher, W. L., and P. U. Rodda, 1969, Edwards Formation (Lower Cretaceous), Texas: Dolomitization in a carbonate platform system: American Association of Petroleum Geologists Bulletin, v. 53, p. 55–72.

Fu, Q., H. Qing, and K. M. Bergman, 2004, Dolomitized calcrete of the middle Devonian Winnipegosis mounds, subsurface of south-central Saskatchewan: Canadian Journal of Sedimentary Geology, v. 168, p. 49–69, doi:10.1016/j.sedgeo.2004.03.007.

Hauwert, N. M., 2009, Groundwater flow and recharge within the Barton Springs segment of the Edwards Aquifer, southern

Travis and northern Hays counties, Texas: Ph.D. Dissertation, University of Texas at Austin, 364 p.

Hopkins, J. H., 1995, Evaluation of ground-water in Texas counties bordering the Rio Grande: Texas Water Development Board Limited Publication 214, Austin, 19 p.

Ji, H., S. Wang, Z. Ouyang, S. Zhang, C. Sun, X. Liu, and D. Zhou, 2004, Geochemistry of red residua underlying dolomites in karst terrains of Yunnan-Guizhou Plateau I; the formation of the Pingba profile: Chemical Geology, v. 203, p. 1–27, doi:10.1016/j.chemgeo.2003.08.012.

Jones, B. S., M. Pleydell, K. C. Ng, and E. J. Ng, 1989, Formation of poikilotopic calcite-dolomite fabrics in the Oligocene-Miocene Bluff Formation of Grand Cayman, British West Indies: Bulletin of Canadian Petroleum Geology, v. 37, p. 255–265.

Kaczmarek, S. E., S. M. Fullmer, and F. Hasiuk, 2015, An universal classification scheme for the microcrystals that host limestone microporosity: Journal of Sedimentary Research, v. 85, p. 1197–1212, doi:10.2110/jsr.2015.79.

Kahle, C. F., 2012, Scanning electron microscopy of pulverulite in the Silurian Lockport Dolomite near Rocky Ridge, OH: Carbonates and Evaporites, v. 27, p. 3–8, doi:10.1007/s13146-011-0076-z.

Kastning, E. H., 1981, Tectonism, fractures, and speleogenesis in the Edwards Plateau, Central Texas, U.S.A, *in* B. F. Beck, ed., Proceedings of the Eighth International Congress of Speleology, Bowling Green, Kentucky, July 18–24, 1981: National Speleological Society, Huntsville, Alabama, v. 2, p. 692–695.

Kastning, E. H., 1983, Relict caves as evidence of landscape and aquifer evolution in a deeply dissected carbonate terrain: Southwest Edwards Plateau, Texas, U.S.A., *in* W. Back and P. E. LaMoreaux, eds., V. T. Stringfield Symposium—Processes in karst hydrology: Journal of Hydrology, v. 61, p. 89–112.

Kastning, E. H., 1984, Hydrogeomorphic evolution of karsted plateaus in response to regional tectonism, in groundwater as a geomorphic agent, *in* R. G. LaFleur, ed., Groundwater as a geomorphic agent: Allen and Unwin, Inc., Boston, Massachusetts, p. 351–382.

Kolb, R. A., 1981, Geology of the Signal Hill quadrangle, Hays and Travis counties, Texas: M.S. Thesis, University of Texas at Austin, 80 p.

Lohmann, K. C., 1988, Geochemical patterns of meteoric diagenetic systems and their application to studies of paleokarst, *in* P. W. Choquette and N. P. James, eds., Paleokarst: Springer-Verlag, New York, p. 58–80.

Loucks, R. G., F. J. Lucia, and L. E. Waite, 2013, Origin and description of the micropore network within the Lower Cretaceous Stuart City Trend tight-gas limestone reservoir in Pawnee Field in South Texas: Gulf Coast Association of Geological Societies Journal, v. 2, p. 29–41, <http://gcags.org/Journal/2013.GCAGS.Journal/GCAGS.Journal.2013.vol2.p29-41.Loucks.et.al.pdf> Last accessed August 1, 2018.

Lucia, F. J., and R. G. Loucks, 2013, Micropores in carbonate mud: Early development and petrophysics: Gulf Coast Association of Geological Societies Journal, v. 2, p. 1–10, <http://gcags.org/Journal/2013.GCAGS.Journal/GCAGS.Journal.2013.vol2.p1-10.Lucia.and.Loucks.pdf> Last accessed August 1, 2018.

Machel, H. G., M. L. Borrero, E. Dembicki, H. Huebscher, P. Luo, and Y. Zhao, 2012, The Grosmont: The world's largest unconventional oil reservoir hosted in carbonate rocks, *in* J. Garland, J. E. Neilson, S. E. Laubach, and K. J. Whidden, eds., Advances in carbonate exploration and reservoir analysis: Geologic Society of London Special Publications, U.K., v. 370, p. 49–81, doi:10.1144/SP370.11.

Mahler, B. J., L. Lynch, and P. C. Bennett, 1999, Mobile sediment in an urbanizing karst aquifer: Implications for contaminant transport: Environmental Geology, v. 39, p. 25–38, doi:10.1007/s002540050.

Martin, R. C., and A. Malahoff, 1965, Some recent Russian studies of ignimbritic rocks: New Zealand Journal of Geology and Geophysics, v. 8, p. 706–737, doi:10.1080/00288306.

Merriam-Wester Dictionary, 2017, <https://www.merriam-webster.com/dictionary/pulverulent> Accessed October 22, 2017.

Mueller, H. W., III, 1975, Centrifugal progradation of carbonate banks: A model for deposition and early diagenesis, Ft. Terrett Formation, Edwards Group, Lower Cretaceous, Central Texas: Ph.D. Dissertation, University of Texas at Austin, 300 p.

Poros, Z., H. G. Machel, A. Mindszenty, and F. Molnár, 2013, Cryogenic powderization of Triassic dolostones in the Buda Hills, Hungary: International Journal of Earth Science, v. 102, p. 1513–1539, doi:10.1007/s00531-013-0883-7.

Révész, K. M., and J. M. Landwehr, 2002, $\delta^{13}C$ and $\delta^{18}O$ isotopic composition of $CaCO_3$ measured by continuous flow isotope ratio mass spectrometry: Statistical evaluation and verification by application to Devils Hole core DH–11 calcite: Rapid Communications in Mass Spectrometry, v. 16, p. 2102–2114, doi:10.1002/rcm.833.

Richards, H. C., and W. H. Bryan, 1933, The problem of the Brisbane tuff: Royal Society (Queensland) Proceedings, v. 45, p. 50–61.

Rose, P. R., 1972, Edwards Group, surface and subsurface, central Texas: Bureau of Economic Geology Report of Investigations 74, Austin, Texas, 198 p.

Rose, P. R., 2016, Late Cretaceous and Tertiary burial history, Central Texas: Gulf Coast Association of Geological Societies Journal, v. 5, p. 141–179, <http://gcags.org/Journal/2016.GCAGS.Journal/2016.GCAGS.Journal.v5.09.p141-179.Rose.pdf> Last accessed August 1, 2018.

Sandberg, P. A., 1983, An oscillating trend in Phanerozoic nonskeletal carbonate mineralogy: Nature, v. 305, p. 19–22, doi:10.1038/305019a0.

Shumard, G. S., 1886, A journal of geological observations along the routes traveled by the expedition between Indianola, Texas, and the Valley of the Mimbres, New Mexico, during the years 1855 and 1856, *in* G. G. Shumard, ed., The geology of western Texas: State Printing Office, Austin, Texas, p. 53–121.

Siegesmund, S., and R. Snethlage, 2011, Stone in architecture; preface, *in* S. Siegesmund and R. Snethlage, eds., Stone in architecture: Springer-Verlag, Berlin, Heidelberg, Germany, p. 97–225, doi:10.1007/ß78-3-642-14475-2.

Spötl, C., and T. W. Vennemann, 2003, Continuous-flow isotope ratio mass spectrometric analysis of carbonate minerals: Rapid Communications in Mass Spectrometry, v. 17, p. 1004–1006, doi:10.1002/rcm.1010.

U.S. Climate Data, 2017, <https://www.usclimatedata.com/climate.php?location=UST> Accessed October 19, 2017.

Volery, C., E. Davaud, A. Foubert, and B. Caline, 2009, Shallow-marine microporous carbonate reservoir rocks in the Middle East: Relationship with seawater Mg/Ca ratio and eustatic sea level: Journal of Petroleum Geology, v. 32, p. 313–325, doi:10.1111/j.1747-5457.2009.00452.x.

Volery, C., 2010, Genesis and diagenesis of microporous micrite: *Thèse de Doctorat* 4205, *University de Genève*, Switzerland, 112 p. <http://archive-ouverte.unige.ch/unige:12122> Last accessed August 1, 2018.

Wikipedia, 2017, Interstate 10 in Texas, <https://en.wikipedia.org/wiki/Interstate_10_in_Texas> Last accessed October 26, 2017.

Willis, J. J., B. E. Lock, K. C. Cornell, and D. A. Ruberg, 2001, An exposed evaporite weld and related deformation structures, Edwards Plateau, I–10 Corridor, Kerrville-Junction-Sonora area, Texas: Gulf Coast Association of Geological Societies Transactions, v. 51, p. 389–397.